Gauss-Jacobi-type quadrature rules for fractional directional integrals*

Guofei Pang[a], Wen Chen[a], K.Y. Sze[b*]

[a] Institute of Soft Matter Mechanics, Department of Engineering Mechanics, Hohai University, Nanjing 210098, China.

[b] Department of Mechanical Engineering, The University of Hong Kong, Pokfulam, Hong Kong, China.

* Part of this work was done when the first author was visiting the University of Hong Kong as a research assistant.

Abstract

Fractional directional integrals are the extensions of the Riemann-Liouville fractional integrals from one- to multi-dimensional spaces and play an important role in extending the fractional differentiation to diverse applications. In numerical evaluation of these integrals, the weakly singular kernels often fail the conventional quadrature rules such as Newton-Cotes and Gauss-Legendre rules. It is noted that these kernels after simple transforms can be taken as the Jacobi weight functions which are related to the weight factors of Gauss-Jacobi and Gauss-Jacobi-Lobatto rules. These rules can evaluate the fractional integrals at high accuracy. Comparisons with the three typical adaptive quadrature rules are presented to illustrate the efficacy of the Gauss-Jacobi-type rules in handling weakly singular kernels of different strengths. Potential applications of the proposed rules in formulating and benchmarking new numerical schemes for generalized fractional diffusion problems are briefly discussed in the final remarking section.

Keywords

Fractional directional integral

Directional derivative

Gauss-Jacobi-Lobatto

Quadrature

Fractional Laplacian

Published in
Computers & Mathematics with Applications
66 (2013) 597-607
dx.doi.org/10.1016/j.camwa.2013.04.020

*Corresponding author.
Email address: kysze@hku.hk

1. Introduction

Recent decades have witnessed a fast growing research on the applications of fractional calculus in diverse science and engineering fields such as physics [1,2,3], rheology [4,5], finance [6,7], acoustics [8,9], fractal geometry [10], hydrology [11,12,13], etc. In particular, by replacing the second-order derivative with a derivative of fractional order $\alpha \in (1,2]$ in the conventional advection-diffusion equation, fractional advection-diffusion equation (FADE) appears to be a promising tool to describe solute transport in groundwater [11]. Solutions of the FADE are the Lévy-stable motions which can describe the super-diffusive flow [12]. For modeling problems in higher spatial dimensions, the fractional diffusion operator in the FADE has been extended to the weighted, fractional directional diffusion operator D_M^α from which the full range of the Lévy-stable motions can be generated [13].

The mathematical complexity of fractional derivatives often makes the analytical solutions of FADEs inaccessible [14]. Hence, the numerical solution techniques are usually resorted to. To test a numerical method for solving FADE, a reference solution with defined source term is needed. Take the 2D problem, i.e.

$$D_M^\alpha u(x,y) + f(x,y) = 0 \tag{1}$$

as an example. It is common that the solution u is pre-fixed and the source term f is numerically computed to satisfy the FADE. With f prescribed, the efficacy of the numerical method can be assessed by comparing its prediction with the pre-fixed u. This paper presents a numerical scheme which can compute f to high accuracy for each discrete point in the computational domain.

Fractional directional integrals are involved in the definition of fractional diffusion term $D_M^\alpha u(\mathbf{x})$ where u is the solute concentration and $\mathbf{x}$ the position vector. To evaluate D_M^α, one must first calculate the fractional directional integrals. Since the fractional directional integration of even the most elementary functions may have non-closed form expression, numerical approximation is often required. The vector Grünward formula [15] is a possible choice. However, its accuracy is only O(h) where h is the grid size. Integration quadrature is another alternative. Owing to the weakly singular kernel in the integrand of the fractional directional integral, the conventional quadrature rules such as Newton-Cotes, Gauss-Legendre rule, and its Kronrod refinement [16] fail to offer adequate accuracy. This constitutes a motivation to seek other quadrature rules which are more accurate and fast-convergent.

Gauss-Jacobi-type quadrature rules are potentially effective tools to evaluate fractional directional integrals. This type of rules takes the Jacobi weight function, which defines the orthogonality of the Jacobi polynomials, as the weight function. For a fractional directional integral, the weakly singular kernel $\varsigma^{\gamma-1}$ ($\gamma \in (0,1)$) in the integrand can be transformed to $(1+\xi)^{\gamma-1}$ which becomes a special case of

the Jacobi weight function $(1-\xi)^{\mu}(1+\xi)^{\lambda}$ for $\mu, \lambda>-1$. Consequently, the singularity of the integrand can be effectively removed.

Section 2 will discuss the definitions of fractional directional operators and their roles in the multi-dimensional fractional spatial operators, followed by Section 3 in which Gauss-Jacobi-type rules and their applications to fractional directional integrals are presented. In Section 4, one- and two-dimensional examples are examined and discussed. Finally, Section 5 remarks on the utility of the proposed rules in formulating and benchmarking numerical schemes for generalized fractional directional diffusion problems.

2. Fractional directional integrals and their applications

This section first introduces how the fractional directional integrals are extended from conventional *n*-fold definite integrals and then defines the fractional directional derivatives. In the last subsection, three typical two-dimensional fractional spatial operators are mentioned.

2.1. Directional integrals

The Cauchy formula [17] can rewrite the left-sided *n*-fold definite integral in a convolution form, i.e.

$$I_{a+}^{n} f(x)=\int_{a}^{x}\int_{a}^{x_n}\cdots\int_{a}^{x_3}\int_{a}^{x_2} f(x_1)dx_1dx_2\cdots dx_{n-1}dx_n=\frac{1}{\Gamma(n)}\int_{a}^{x}(x-\xi)^{n-1} f(\xi)d\xi \tag{2}$$

in which $f(x)$ is defined on $[a,b]$, n is a positive integer and $\Gamma(z)$ the gamma function. Similarly, the right-sided integral reads

$$I_{b-}^{n} f(x)=\int_{x}^{b}\int_{x_n}^{b}\cdots\int_{x_3}^{b}\int_{x_2}^{b} f(x_1)dx_1dx_2\cdots dx_{n-1}dx_n=\frac{1}{\Gamma(n)}\int_{x}^{b}(\xi-x)^{n-1} f(\xi)d\xi\,. \tag{3}$$

Applying the transforms $\varsigma=\pm(x-\xi)$ to formulas (2) and (3) produces

$$I_{0}^{n} f(x)=\frac{1}{\Gamma(n)}\int_{0}^{x-a}\varsigma^{n-1} f(x-\varsigma\cos 0)d\varsigma\,, \tag{4}$$

$$I_{\pi}^{n} f(x)=\frac{1}{\Gamma(n)}\int_{0}^{b-x}\varsigma^{n-1} f(x-\varsigma\cos\pi)d\varsigma, x\in[a,b]\,. \tag{5}$$

The subscripts of the above integration operators "I^n" denote the integration direction $\theta\in[0,2\pi)$. The integration operators in (4) and (5) can be generalized to rectangular domain

$$I_\theta^n g(x,y) = \frac{1}{\Gamma(n)} \int_0^{d(x,y,\theta)} \varsigma^{n-1} g(x-\varsigma\cos\theta, y-\varsigma\sin\theta) d\varsigma, \quad (x,y) \in \Omega = [a,b]\times[c,d], \theta \in [0,2\pi). \tag{6}$$

The upper integration limit $d(x,y,\theta)$ is termed as the "backward distance" of point (x,y) to $\partial\Omega$ along the direction $\boldsymbol{\theta}=\{\cos\theta,\sin\theta\}^T$, as seen in Fig.1. Similarly, the directional integral in three-dimensional space can be defined as

$$I_{\boldsymbol{\theta}}^n h(x,y,z) = \frac{1}{\Gamma(n)} \int_0^{d(x,y,z,\boldsymbol{\theta})} \varsigma^{n-1} h(x-\varsigma\theta_1, y-\varsigma\theta_2, z-\varsigma\theta_3) d\varsigma, \quad (x,y,z) \in \Omega = [a,b]\times[c,d]\times[e,f], \boldsymbol{\theta} = \{\theta_1,\theta_2,\theta_3\}^T, \|\boldsymbol{\theta}\|_2 = 1. \tag{7}$$

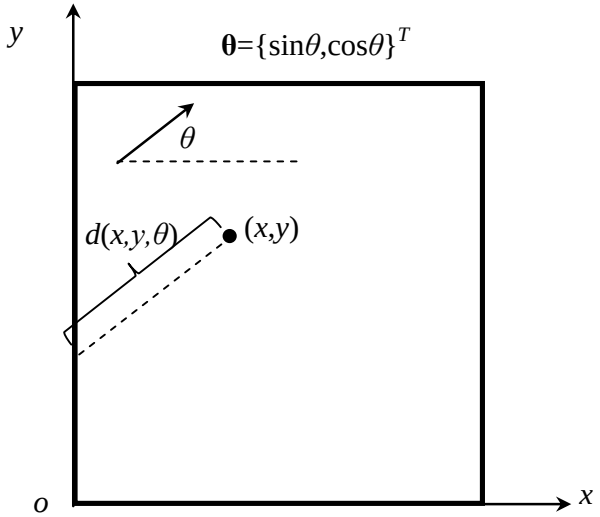

Fig.1. The backward distance $d(x,y,\theta)$ of node (x,y) to the boundary of a rectangle in the direction $\boldsymbol{\theta}$.

For simplifying discussion, we shall concentrate on the integrations in one- and two- dimensional spaces. Substituting n in integral (6) with a fraction $\gamma \in (n\text{-}1,n)$ yields the fractional directional integrals, i.e.

$$I_\theta^\gamma g(x,y) = \frac{1}{\Gamma(\gamma)} \int_0^{d(x,y,\theta)} \varsigma^{\gamma-1} g(x-\varsigma\cos\theta, y-\varsigma\sin\theta) d\varsigma\,. \tag{8}$$

Through integration by parts, one can prove that I_θ^γ becomes the identity operator I as $\gamma\to 0$. When θ equals 0 and π, integral (8) can be recovered to left- and right-sided Riemann-Liouville integrals [17], respectively.

2.2. Compounding the directional differentiation and fractional directional integration operators

The *n*-th order directional derivative of $g(x, y)$ is defined as

$$D_\theta^n g(x,y) = \left(\frac{\partial}{\partial x}\cos\theta + \frac{\partial}{\partial y}\sin\theta \right)^n g(x,y). \tag{9}$$

The operators in (8) and (9) can be compounded in two different ways which leads to the Riemann-Liouville and Caputo fractional directional operators, namely

$$\begin{cases} D_\theta^\alpha g(x,y) = D_\theta^n I_\theta^{n-\alpha} g(x,y) & \text{(Riemann - Liouville)}, \\ {}^{*}D_\theta^\alpha g(x,y) = I_\theta^{n-\alpha} D_\theta^n g(x,y) & \text{(Caputo)}, \end{cases} \quad \alpha \in (n-1, n). \tag{10}$$

The fractional directional integration operators possess the following properties similar to those of I_0^γ or I_{a+}^γ [18], i.e.

$$I_\theta^{\gamma_1} I_\theta^{\gamma_2} = I_\theta^{\gamma_2} I_\theta^{\gamma_1} = I_\theta^{\gamma_1+\gamma_2}, \tag{11}$$

$$\int_\Omega I_\theta^\gamma u v d\Omega = \int_\Omega u I_{\theta+\pi}^\gamma v d\Omega, \tag{12}$$

and the integration and differentiation operators of the same order satisfy

$$D_\theta^\gamma I_\theta^\gamma = I. \tag{13}$$

More properties of the fractional directional integrals and derivatives can be found in [18].

2.3. Riesz potential, fractional Laplacian and generalized fractional diffusion operator

The formulation of the Laplacian of a fractional order generally depends on the Fourier transforms [19]:

$$(-\Delta)^{\alpha/2} \varphi(\mathbf{x}) = \mathcal{F}^{-1} \left\| \boldsymbol{\kappa} \right\|_2^\alpha \tag{14}$$

with $\mathbf{x}, \boldsymbol{\kappa} \in \mathbb{R}^2$.

For $\alpha<0$, the left hand side of (14) is the Riesz potential [19]

$$I^{-\alpha} \varphi(\mathbf{x}) = (-\Delta)^{\alpha/2} \varphi(\mathbf{x}) = \frac{1}{\eta_2(-\alpha)} \int_{\mathbb{R}^2} \frac{\varphi(\mathbf{y}) d\mathbf{y}}{\left\| \mathbf{x} - \mathbf{y} \right\|_2^{2+\alpha}}, -\alpha \neq 2, 4, 6, \ldots \tag{15}$$

with $\eta_2(-\alpha)$ defined in [Eq.(25.26) ,19]. Using the polar coordinates and the definition in (8), one can rewrite (15) in the following form [Eq. (25.34), 19]:

$$I^{-\alpha}\varphi(x,y)=\frac{\Gamma(\frac{1-\alpha}{2})\Gamma(\frac{2+\alpha}{2})}{2\pi^{3/2}}\int_0^{2\pi} I_\theta^{-\alpha}\varphi(x,y)d\theta,-\alpha\neq 2,4,6,\ldots. \tag{16}$$

Eq.(16) shows that the Riesz potential can be interpreted as an integration of fractional directional integral $I_\theta^{-\alpha}\varphi(x,y)$. Here, the backward distance $d(x,y,\theta)$ in $I_\theta^{-\alpha}\varphi(x,y)$ is ∞.

For $\alpha>0$, the fractional Laplacian can similarly be defined as an integration of fractional directional derivative, namely [Eq. (26.24) ,19]

$$\left(-\Delta\right)^{\alpha/2}\varphi(x,y)=-\frac{\Gamma(-\alpha)\sin(\alpha\pi/2)}{\beta_2(\alpha)}\int_0^{2\pi} D_\theta^{\alpha}\varphi(x,y)d\theta \tag{17}$$

with $\beta_2(\alpha)$ defined in [Eq. (26.8),19]. Using basic relationships of the gamma function [20], i.e.

$$\begin{aligned}&\Gamma(z)=(z-1)\Gamma(z-1),\mathrm{Re}(z)>0,\\&\Gamma(z)\Gamma(1-z)=\frac{\pi}{\sin(\pi z)},z\notin \mathbb{Z};0<\mathrm{Re}(z)<1,\\&\Gamma(2z)=\frac{2^{2z-1}}{\sqrt{\pi}}\Gamma(z)\Gamma(z+\frac{1}{2}),z\in \mathbb{C},\end{aligned} \tag{18}$$

(17) can be written in a form similar to (16)

$$\left(-\Delta\right)^{\alpha/2}\varphi(x,y)=\frac{\Gamma(\frac{1-\alpha}{2})\Gamma(\frac{2+\alpha}{2})}{2\pi^{3/2}}\int_0^{2\pi} D_\theta^{\alpha}\varphi(x,y)d\theta. \tag{19}$$

From (16) and (19), one can see that the Laplacian of a fractional order can be expressed in terms of an integration of the fractional directional integral or derivative. Incidentally, another type of definition of fractional Laplacian, which helps to model the acoustic attenuation in lossy media exhibiting arbitrary frequency power-law dependency, can be found in [30].

Assigning a probability weight to each direction θ in (19) will yield a generalized fractional diffusion operator [13]:

$$D_M^{\alpha}\varphi(x,y)=\int_0^{2\pi} D_\theta^{\alpha}\varphi(x,y)M(d\theta),\ (1<\alpha\leq 2) \tag{20}$$

with the finite probability measure $M(d\theta)$. In compliance with the differential order in FADE, $\alpha\in(1,2]$ is limited. When $M(d\theta)$ is uniform or $M(d\theta)=1/(2\pi)d\theta$, the relationships in (18) lead to the following relation between the fractional Laplacian and the generalized fractional diffusion operator

$$D_M^{\alpha}\varphi(x,y)=\frac{\sqrt{\pi}}{\Gamma(\frac{1-\alpha}{2})\Gamma(\frac{2+\alpha}{2})}(-\Delta)^{\alpha/2}\varphi(x,y),\alpha\in(1,2]. \tag{21}$$

A trivial case of (21) is $D_M^2=0.5\Delta$. It can be seen from (21) that the fractional Laplacian is simply a special case of the generalized fractional diffusion operator with a uniform *M*.

3. Gauss-Jacobi-type rules

The Gauss-Jacobi-type rules approximate the integral of the form

$$\int_{-1}^{+1} w^{(\mu,\lambda)}(\xi)\,f(\xi)d\xi\,,\ \mu,\lambda\text{>-1} \tag{22}$$

in which *f* is a sufficiently smooth non-singular function and

$$w^{(\mu,\lambda)}(\xi)=(1-\xi)^{\mu}(1+\xi)^{\lambda},\ \mu,\lambda>-1 \tag{23}$$

is the Jacobi weight function. The quadrature points are the zeros of the Jacobi polynomials to be discussed in the following subsection. The approach in [21] is employed here to solve the zeros.

3.1. Jacobi polynomials and their zeros

Jacobi polynomials $P_n^{(\mu,\lambda)}$ of degree *n* defined in [-1,+1] satisfy the following orthogonal condition

$$\int_{-1}^{+1} w^{(\mu,\lambda)}(x)P_m^{(\mu,\lambda)}(x)P_n^{(\mu,\lambda)}(x)dx=C_{n,\mu,\lambda}\delta_{mn} \tag{24}$$

where

$$C_{n,\mu,\lambda}=\frac{2^{\mu+\lambda+1}}{2n+\mu+\lambda+1}\frac{\Gamma(n+\mu+1)\,\Gamma(n+\lambda+1)}{\Gamma(n+\mu+\lambda+1)n!}. \tag{25}$$

The Jacobi polynomials $P_N^{(\mu,\lambda)}$ can be obtained by the following recursive relation

$$\begin{aligned}&P_n^{(\mu,\lambda)}(x)=(a_n x+b_n)P_{n-1}^{(\mu,\lambda)}(x)-c_n P_{n-2}^{(\mu,\lambda)}(x),\ n=1,2,...,N\\&P_{-1}^{(\mu,\lambda)}(x)=0,P_0^{(\mu,\lambda)}(x)=1\end{aligned} \tag{26}$$

with

$$(a_n, b_n) = \begin{cases} \dfrac{2n+\mu+\lambda-1}{2n(n+\mu+\lambda)}(2n+\mu+\lambda, \dfrac{\mu^2-\lambda^2}{2n+\mu+\lambda-2}), & \mu+\lambda \neq -1 \\ \dfrac{1}{n}(2n-1, \dfrac{\mu^2-\lambda^2}{2n-3}), & n \geq 2, \mu+\lambda = -1, \\ \dfrac{1}{2}(1, \lambda^2-\mu^2), & n = 1, \mu+\lambda = -1, \end{cases} \tag{27}$$

$$c_n = \frac{(n+\mu-1)(n+\lambda-1)(2n+\mu+\lambda)}{n(n+\mu+\lambda)(2n+\mu+\lambda-2)}, \; n \geq 2. \tag{28}$$

The equation system in (26) can be expressed in a matrix-vector form as [21,22]

$$x\begin{Bmatrix} \tilde{P}_0^{(\mu,\lambda)}(x) \\ \tilde{P}_1^{(\mu,\lambda)}(x) \\ \vdots \\ \vdots \\ \tilde{P}_{N-2}^{(\mu,\lambda)}(x) \\ \tilde{P}_{N-1}^{(\mu,\lambda)}(x) \end{Bmatrix} = \begin{bmatrix} A_1 & B_1 & & & & 0 \\ B_1 & A_2 & B_2 & & & \\ & B_2 & \ddots & \ddots & & \\ & & \ddots & \ddots & \ddots & \\ & & & \ddots & A_{N-1} & B_{N-1} \\ 0 & & & & B_{N-1} & A_N \end{bmatrix} \begin{Bmatrix} \tilde{P}_0^{(\mu,\lambda)}(x) \\ \tilde{P}_1^{(\mu,\lambda)}(x) \\ \vdots \\ \vdots \\ \tilde{P}_{N-2}^{(\mu,\lambda)}(x) \\ \tilde{P}_{N-1}^{(\mu,\lambda)}(x) \end{Bmatrix} + \begin{Bmatrix} 0 \\ 0 \\ \vdots \\ \vdots \\ 0 \\ B_N \tilde{P}_N^{(\mu,\lambda)}(x) \end{Bmatrix} \tag{29}$$

in which $A_n = -b_n / a_n$, $B_n = \sqrt{c_{n+1} / a_n a_{n+1}}$ and $\tilde{P}_n^{(\mu,\lambda)} = P_n^{(\mu,\lambda)} / \sqrt{C_{n,\mu,\lambda}}$. One can see that x_i is the zero of $P_N^{(\mu,\lambda)}(x)$ iff x_i is the eigenvalue of the above tridiagonal matrix.

3.2. Gauss-Jacobi rule

In the Gauss-Jacobi rule, the weighted integration in (22) is evaluated by

$$\int_{-1}^{+1} f(\xi) w^{(\mu,\lambda)}(\xi) d\xi = \sum_{k=1}^{N} \omega_k f(\xi_k) \tag{30}$$

and the error [23] is

$$\frac{f^{(2N)}(\eta)}{(2N)!} \int_{-1}^{+1} \left[\prod_{k=1}^{N} (\xi - \xi_k) \right]^2 (1-\xi)^{\mu} (1+\xi)^{\lambda} d\xi, \; \eta \in (-1, +1). \tag{31}$$

Obviously, the rule is exact for polynomials of degree up to 2*N*-1. The quadrature points ξ_k are the zeros of $P_N^{(\mu,\lambda)}(\xi)$. And according to [21], the weight factors ω_k are determined by

$$\omega_k = c_0 q_k^2 \tag{32}$$

where q_k is the first component of the normalized (unit) eigenvector corresponding to the k-th eigenvalue ξ_k and

$$c_0 = \int_{-1}^{+1} w^{(\mu,\lambda)}(\xi) d\xi = \int_{-1}^{+1} (1-\xi)^{\mu}(1+\xi)^{\lambda} d\xi = 2^{\mu+\lambda+1} B(\mu+1, \lambda+1) \tag{33}$$

where $B(\cdot,\cdot)$ is the beta function. As a matter of fact, the commonly used Gauss-Legendre rule can be regarded as a special case of the Gauss-Jacobi rule with weight function $1=(1-\xi)^0(1+\xi)^0$, i.e. $\mu = \lambda = 0$.

3.3 Gauss-Jacobi-Lobatto rule

In the Gauss-Jacobi-Lobatto rule, the weighted integration in (22) is evaluated by

$$\int_{-1}^{+1} f(\xi)(1-\xi)^{\mu}(1+\xi)^{\lambda} d\xi = \omega_1 f(-1) + \sum_{k=2}^{N+1} \omega_k f(\xi_k) + \omega_{N+2} f(1) \tag{34}$$

and the error [23] is

$$\frac{f^{(2N+2)}(\eta)}{(2N+2)!} \int_{-1}^{1} (\xi^2 - 1) \left[\prod_{k=2}^{N+1} (\xi - \xi_k) \right]^2 (1-\xi)^{\mu}(1+\xi)^{\lambda} d\xi, \eta \in (-1, +1) \tag{35}$$

It can be seen that the quadrature points include the integration limits and the rule is exact for polynomials of degree up to $2N+1$. The interior quadrature points ξ_k are zeros of $P_N^{(\mu+1,\lambda+1)}(\xi)$. There are three equivalent sets of formulas for the weight factors ω_k [24,25,26], among which the one by Zheng and Huang [25] is as follows

$$\begin{cases} \omega_1^{\mu,\lambda} = 2^{\mu+\lambda+1} \dfrac{\Gamma(\mu+2)\,\Gamma(\lambda+1)}{\Gamma(\mu+\lambda+3)} \dfrac{\binom{N+\mu+1}{N}}{\binom{N+\lambda+1}{N}\binom{N+\mu+\lambda+2}{N}}, \\ \omega_k^{\mu,\lambda} = \dfrac{2^{\mu+\lambda+1}\,\Gamma(\mu+N+2)\,\Gamma(\lambda+N+2)}{(N+1)^2\,\Gamma(N+1)\,\Gamma(\mu+\lambda+N+3)\left[P_{N+1}^{(\mu,\lambda)}(\xi_k)\right]^2}, \; k = 2,3,\ldots,N+1, \\ \omega_{N+2}^{\mu,\lambda} = \omega_1^{\lambda,\mu}. \end{cases} \tag{36}$$

For the purpose of reducing the accumulative numerical errors for a large N, $P_{N+1}^{(\mu,\lambda)}(\xi_k)$ in (36) is evaluated by

$$P_{N+1}^{(\mu,\lambda)}(\xi_k) = K_{N+1}^{(\mu,\lambda)} \prod_{i=1}^{N+1} (\xi_k - \tilde{x}_i) \tag{37}$$

with the zeros $\tilde{x}_i$ of $P_{N+1}^{(\mu,\lambda)}$ from the computed eigenvalues and the leading coefficient $K_{N+1}^{(\mu,\lambda)}$ derived from (26).

3.4 Gauss-Jacobi-type rules for fractional directional integrals

Returning to the fractional directional integral in (8), the transform $\varsigma=(d/2)(1+\xi)$ allows us to rewrite (8) as

$$I_\theta^\gamma g(x,y)=\frac{1}{\Gamma(\gamma)}\left(\frac{d(x,y,\theta)}{2}\right)^\gamma \int_{-1}^{1}(1+\xi)^{\gamma-1}\tilde{g}(\varsigma;x,y,\theta)d\xi,\ \ \gamma\in(0,1) \tag{38}$$

where

$$\tilde{g}(\varsigma;x,y,\theta)=g(x-\frac{d(x,y,\theta)}{2}(1+\xi)\cos\theta, y-\frac{d(x,y,\theta)}{2}(1+\xi)\sin\theta)\,. \tag{39}$$

Here the weakly singular term $(1+\xi)^{\gamma-1}$ in (38) can be treated as the weight functions with $\mu = 0$ and $\lambda = \gamma-1$ in (30) and (34). Accordingly, (30) or (34) can be adopted to evaluate (38). Our Matlab codes for computing the quadrature points and weight factors of the Gauss-Jacobi-type rules based on any input μ- and λ- values larger than -1 can be accessed at http://www.ismm.ac.cn/download.html.

4. Numerical results and discussions

In Section 4.1**,** we consider the Riemann-Liouville integration I_{a+}^γ of two elementary functions. I_{a+}^γ can be seen as a directional integration operator along the positive *x*-axis, i.e. $I_{a+}^\gamma = I_0^\gamma$. We compare the approximations of the Gauss-Jacobi quadrature (GJ) and Gauss-Jacobi-Lobatto quadrature (GJL) with those from the Matlab build-in functions *quad*, *quadl* and *quadgk* which offer the adaptive Simpson quadrature, adaptive Lobatto quadrature [27] and adaptive Gauss-Kronrod quadrature [28], respectively. To avoid the endpoint infinities, *quad* and *quadl* replace the function evaluations at the endpoints by the values computed at their close neighborhoods. On the other hand, *quadgk* does not sample the integrand at the endpoints and is recommended for integral with moderate endpoint singularity [28]. An integration interval/subinterval would be kept being subdivided into shorter intervals unless the integral over the subinterval before and after a subdivision is smaller than a priori tolerance. The following warning messages may be returned by *quad*, *quadl* and *quadgk*:

Table 1. *Err* of GJL, GJ for different γ and numbers of quadrature points.

γ		Number of quadrature points							
		1	2	3	4	5	6	7	8
0.25	GJL	_	4.61e-1	5.92e-2	3.61e-3	1.25e-4	2.90e-6	4.68e-8	7.84e-10
	GJ	6.94e-1	7.08e-2	4.10e-3	1.43e-4	3.22e-6	5.16e-8	6.38e-10	4.16e-10
0.50	GJL	_	9.50e-1	1.13e-1	6.40e-3	2.17e-4	4.87e-6	7.72e-8	9.11e-10
	GJ	9.13e-1	1.03e-1	6.23e-3	2.14e-4	4.86e-6	7.75e-8	1.00e-9	2.95e-10
0.75	GJL	_	1.37e+0	1.63e-1	8.81e-3	2.84e-4	6.09e-6	9.24e-8	1.09e-9
	GJ	9.35e-1	1.19e-1	7.12e-3	2.41e-4	5.35e-6	8.35e-8	1.01e-9	2.96e-10

W1: the minimal step size is reached

(For *quad* and *quadl*, W1 will be returned when the shortest subinterval reaches *eps*×(*b*-*a*)/1024 where *a* and *b* are the integration limits and *eps* ≈ 2.26×10^{-16}. For *quadgk*, W1 will be returned when $|x_i\text{-}x_{i+1}| \le 100\ eps\ x_{i+1}$ in which x_i and x_{i+1} are the real non-normalized coordinate of two consecutive integration points)

W2: the maximum number of function evaluations is reached

(For *quad* and *quadl*, the number is 10000. For *quadgk*, W2 is returned when the total number of subintervals exceeds control parameter MaxIntervalCount which is 650 in default.)

W3: infinite value is encountered in a function evaluation.

In Section 4.2, the discretization of the generalized fractional diffusion operator mentioned in Section 2.3 would be investigated by using the approximations of the fractional directional integrals in two-dimensional space.

4.1 Riemann-Liouville fractional integration of sin(x)and $x^{\gamma-1}$cos (2x)

4.1.1 sin(x)

The fractional integral being considered is

$$I_0^{\gamma}\sin(x)=\frac{1}{\Gamma(\gamma)}\int_0^x \varsigma^{\gamma-1}\sin(x-\varsigma)d\varsigma\ ,\ x\in[0,2\pi],\gamma\in(0,1)\,. \tag{40}$$

The explicit expression of the integral is [Table 9.1, 19]:

$$I_0^{\gamma}\sin(x)=\frac{x^{\gamma}}{2i\,\Gamma(\gamma+1)}\left[{}_1F_1(1;\gamma+1;ix)-{}_1F_1(1;\gamma+1;-ix)\right] \tag{41}$$

where *i* denotes $\sqrt{-1}$ and ${}_1F_1$ is the generalized hyper-geometric function defined as

$$ {}_1F_1(p;q;z)=\sum_{k=0}^{\infty}\frac{(p)_k z^k}{(q)_k}. \tag{42}$$

In (42), $(a)_k=a(a+1)\cdots(a+k-1)$. The function ${}_1F_1$ is available in some computational software such as Matlab and Maple. The test point set $\{x_k = k\pi/8,\ k = 0,1,2,\ldots,16\}$ is considered. Denoting the exact and quadrature results at x_k by respectively R_k and Q_k, the following normalized error is computed:

$$ Err=\sqrt{\frac{\sum_{k=0}^{16}\left(Q_k-R_k\right)^2}{\sum_{k=0}^{16}R_k^2}}. \tag{43}$$

Err of GJL (μ=0, λ=γ-1) and GJ (μ=0, λ=γ-1) are listed in Table 1. *Err* of the adaptive methods with the error tolerance 10^{-6} and 10^{-10} are listed in Table 2. The "(W*n*)" behind the data in Table 2 are the warning messages, if any, returned by Matlab and "Inf" indicates that the returned value of the integration is infinite.

From the two tables, it can be seen that the Gauss-Jacobi-type rules can handle singularities of different strengths controlled by $0<\gamma<1$, whilst the adaptive methods cannot. The influence of the strong singularity on the adaptive methods is obvious. To summarize, the adaptive methods fail more readily when the singularity is strong and when the preset tolerance is high. Among them, *quadgk* is the best option as recommended by the Matlab manual.

Table 2. *Err* of adaptive methods with error tolerances 10^{-6} and 10^{-10}.

	Error tolerance = 10^{-6}			Error tolerance = 10^{-10}		
	γ = 0.25	γ = 0.5	γ = 0.75	γ = 0.25	γ = 0.5	γ = 0.75
quad	1.29e-4(W1)	1.21e-5	1.16e-5	1.38e-5(W1)	1.43e-8	2.98e-10
quadl	2.70e-5	4.52e-7	9.84e-7	2.54e-5(W1)	5.65e-10(W1)	2.96e-10
quadgk	Inf(W3)	2.96e-10	3.38e-8	Inf(W3)	2.96e-10	2.98e-10

Table 3. *Err* of GJL, GJ rules for different γ and numbers of quadrature points.

γ		Number of quadrature points							
		1	2	3	4	5	6	7	8
0.01	GJL	_	4.41e-3	1.52e-3	1.32e-4	5.94e-6	1.64e-7	3.08e-9	4.18e-11
	GJ	2.87e-1	2.52e-3	1.88e-4	7.74e-6	2.02e-7	3.66e-9	4.85e-11	4.90e-13
0.1	GJL	_	5.54e-2	1.89e-2	1.65e-3	7.37e-5	2.04e-6	3.82e-8	5.19e-10
	GJ	3.80e-1	2.74e-2	2.25e-3	9.10e-5	2.41e-6	4.39e-8	5.85e-10	5.93e-12
0.3	GJL	_	2.98e-1	9.55e-2	8.21e-3	3.65e-4	1.00e-5	1.88e-7	2.55e-9
	GJ	7.34e-1	1.12e-1	9.31e-3	4.03e-4	1.09e-5	2.00e-7	2.70e-9	2.76e-11

Table 4. *Err* of adaptive methods with error tolerances 10^{-6} and 10^{-10}

	Error tolerance = 10^{-6}			Error tolerance = 10^{-10}		
	$\gamma = 0.01$	$\gamma = 0.1$	$\gamma = 0.3$	$\gamma = 0.01$	$\gamma = 0.1$	$\gamma = 0.3$
quad	Inf(W3)	Inf(W3)	1.56e-5	Inf(W3)	Inf(W3)	Inf(W3)
quadl	Inf(W3)	Inf(W3)	Inf(W3)	2.60e+3(W2)	1.00e+3(W2)	Inf(W3)
quadgk	6.90e-1(W1)	2.41e-2(W1)	1.14e-5(W1)	6.90e-1(W1)	2.41-1(W1)	1.14e-5(W1)

4.1.2 $x^{\gamma-1}\cos(2x)$

The fractional integral being considered is

$$I_0^{\gamma}\left(x^{\gamma-1}\cos(2x)\right)=\frac{1}{\Gamma(\gamma)}\int_0^x \varsigma^{\gamma-1}(x-\varsigma)^{\gamma-1}\cos[2(x-\varsigma)]d\varsigma, x\in[0,\pi], \gamma\in(0,1). \tag{44}$$

The explicit expression for the integral is [Table 9.1, 19]:

$$I_0^{\gamma}\left(x^{\gamma-1}\cos(2x)\right)=(\frac{x}{2})^{0.5-\gamma}\sqrt{\pi}\cos(x)J_{\gamma-0.5}(x) \tag{45}$$

in which $J_\beta(x)$ denotes the Bessel function of the first kind. Unlike (40), the integrand of (45) is singular at both endpoints. With the transform $\varsigma=(x/2)(1+\xi)$, (44) becomes

$$I_0^{\gamma}\left(x^{\gamma-1}\cos(2x)\right)=\frac{1}{\Gamma(\gamma)}(\frac{x}{2})^{2\gamma-1}\int_{-1}^{1}(1-\xi)^{\gamma-1}(1+\xi)^{\gamma-1}\cos[x(1-\xi)]d\xi \tag{46}$$

To take proper account of the singularities, the parameters for GJL and GJ are $\mu = \lambda = \gamma$-1. With the test point set $\{x_k=k\pi/16,\ k=0,1,2,\ldots,16\}$, *Err* defined in (43) is computed for GJ and GJL. We only consider relatively strong singularities given by $\gamma = 0.01$, 0.1 and 0.3. The results are listed in Table 3. The errors of the adaptive methods are shown in Table 4.

This example is more challenging than the previous one for the adaptive methods as the integrand is singular at both endpoints. Since only the relatively strong singularities are considered, the adaptive rules fail in all combinations of singularities and error tolerances. All the three warning messages can be seen in Table 4. On the other hand, Gauss-Jacobi-type rules still give very accurate approximants.

4.2 Fractional spatial differentiation of $x^2(1-x)^2y^2(1-y)^2$

Owing to the hyper-singularity in the generalized fractional diffusion term (20), for convenience of computation, the following Caputo-type counterpart is considered

$$ {}^{*}D_{M}^{\alpha}\varphi(x,y)=\int_{0}^{2\pi}{}^{*}D_{\theta}^{\alpha}\varphi(x,y)M(d\theta)\ ,\quad 1<\alpha\le 2\ ,\ (x,y)\in[0,1]^2. \tag{47} $$

Table 5. *Err* of the approximants of fractional diffusion term (48) for different GL rules applied to the subinterval of θ.

Rule for integration w.r.t.ς	Number of quadrature points in GL for each subinterval of θ						
	4	8	12	16	20	24	28
4-point GJL	1.62e-2	1.62e-2	1.62e-2	1.62e-2	1.62e-2	1.62e-2	1.62e-2
5-point GJL	3.49e-5	5.69e-7	7.40e-9	6.60e-10	2.46e-11	1.14e-12	9.95e-13
3-point GJ	1.39e-2	1.39e-2	1.39e-2	1.39e-2	1.39e-2	1.39e-2	1.39e-2
4-point GJ	3.49e-5	5.69e-7	7.40e-9	6.60e-10	2.46e-11	1.14e-12	9.97e-13

In this example, α=1.5, $\varphi(x,y)=x^2(1-x)^2y^2(1-y)^2$ and $M(d\theta)=1/(2\pi)\mathrm{d}\theta$ are taken. The backward distance for any internal node (x,y) is

$$ d(x,y,\theta)=\begin{cases} \dfrac{x}{\cos\theta},\theta\in\left[-\phi,\arctan(\dfrac{y}{x})\right), \\ \dfrac{y}{\sin\theta},\theta\in\left[\arctan(\dfrac{y}{x}),\pi+\arctan(\dfrac{y}{x-1})\right), \\ \dfrac{x-1}{\cos\theta},\theta\in\left[\pi+\arctan(\dfrac{y}{x-1}),\pi+\arctan(\dfrac{y-1}{x-1})\right), \\ \dfrac{y-1}{\sin\theta},\theta\in\left[\pi+\arctan(\dfrac{y-1}{x-1}),2\pi-\phi\right) \end{cases} \tag{48} $$

in which ϕ = arctan((1-y)/x) $\in$ (0, π/2). It is trivial that d is not C^1 at the θs defined by the lines joining (x,y) and the four corners of the square domain $[0,1]^2$. Without loss of generality, the diffusion term to be evaluated can be expressed as:

$$ {}^{*}D_{M}^{1.5}\varphi(x,y)=\frac{1}{2\pi\,\Gamma(0.5)}\int_{-\phi}^{2\pi-\phi}\int_{0}^{d(x,y,\theta)}\varsigma^{-0.5}v(x-\varsigma\cos\theta,y-\varsigma\sin\theta)d\varsigma\,d\theta \tag{49} $$

in which $v(x,y)=D_{\theta}^{2}\varphi(x,y)$ and the integration limits for θ have been shifted from (0,2π) to (-ϕ, 2π-ϕ). The integration with respect to θ is handled by dividing [-ϕ,2π-ϕ] into four subintervals according to (48).

The following normalized error for the set of test points $\{(x_i, y_i)=(i/8, j/8), i,j = 1,2,\ldots,7\}$ is computed by

$$Err = \sqrt{\frac{\sum_{i,j=1}^{7}\left(Q_{ij}-P_{ij}\right)^2}{\sum_{i,j=1}^{7}P_{ij}^2}}. \tag{50}$$

For Q_{ij}, the integration with respect to ς is calculated by the GJ or GJL whilst the integration with respect to θ is done by applying Gauss-Legendre quadrature (GL) to each of the four subintervals of θ. Based on the error terms (31), (35) and the fact that $\varphi(x,y)$ is a polynomial of degree 8 on arbitrary oblique line, 4-point GJ and 5-point GJL are exact for the integration with respect to ς. P_{ij} is the reference solution in which the integration with respect to ς is analytically evaluated whilst the integration with respect to θ is numerically done with successively higher order GL rule until the result has been highly converged. The errors by using GJL/GJ and GL to evaluate (49) are tabulated in Table 5. Very high accuracy can be yielded by judiciously combining GJL/GJ and GL in the two integrations with respect to ς and θ, respectively.

Next, we examine the definition of ${}^{*}D_M^{\alpha}$ by illustrating that the fractional diffusion term can be recovered to the conventional diffusion term, i.e.

$$\lim_{\alpha\to 2} {}^{*}D_M^{\alpha} = {}^{*}D_M^{2}. \tag{51}$$

From the definitions of two fractional directional derivatives in (10) and $I_{\theta}^{0} = I$, it can be proven that ${}^{*}D_M^{2} = D_M^{2}$. Only the special case of (51) in which $M(d\theta)=1/(2\pi)d\theta$ is considered. By (21), one gets ${}^{*}D_M^{2} = D_M^{2} = 0.5\Delta$. Thus, (51) can be illustrated through

$$\lim_{\alpha\to 2} {}^{*}D_M^{\alpha}\varphi(x,y) = 0.5\Delta\varphi(x,y). \tag{52}$$

The following normalized difference is computed

$$Dif = \sqrt{\frac{\sum_{i,j=1}^{15}\left(Q_{ij}-0.5\Delta\varphi\left(i/16,\, j/16\right)\right)^2}{\sum_{i,j=1}^{15}\left(0.5\Delta\varphi\left(i/16,\, j/16\right)\right)^2}} \tag{53}$$

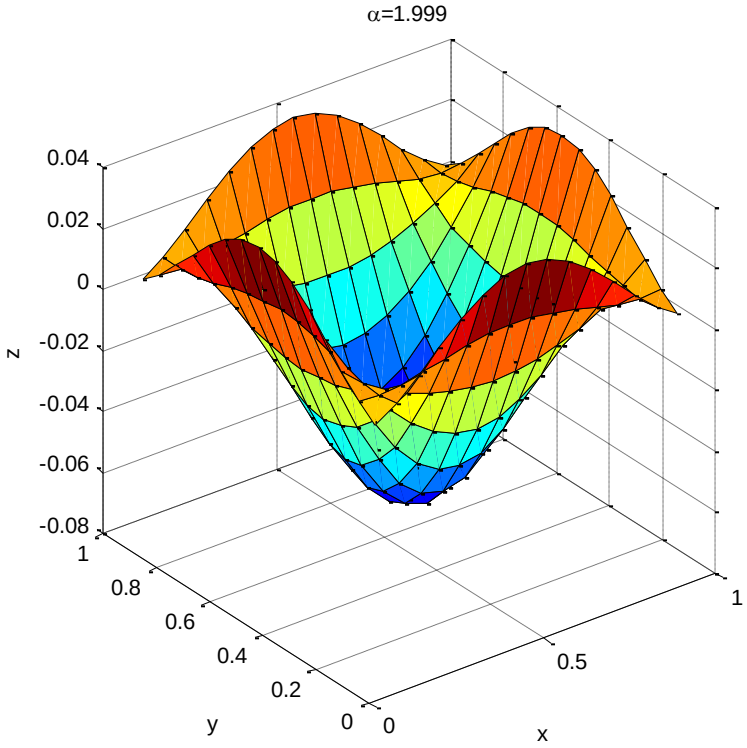

Fig.2. Surface plot of $z = {}^{*}D_{M}^{1.999}\varphi(x, y)$.

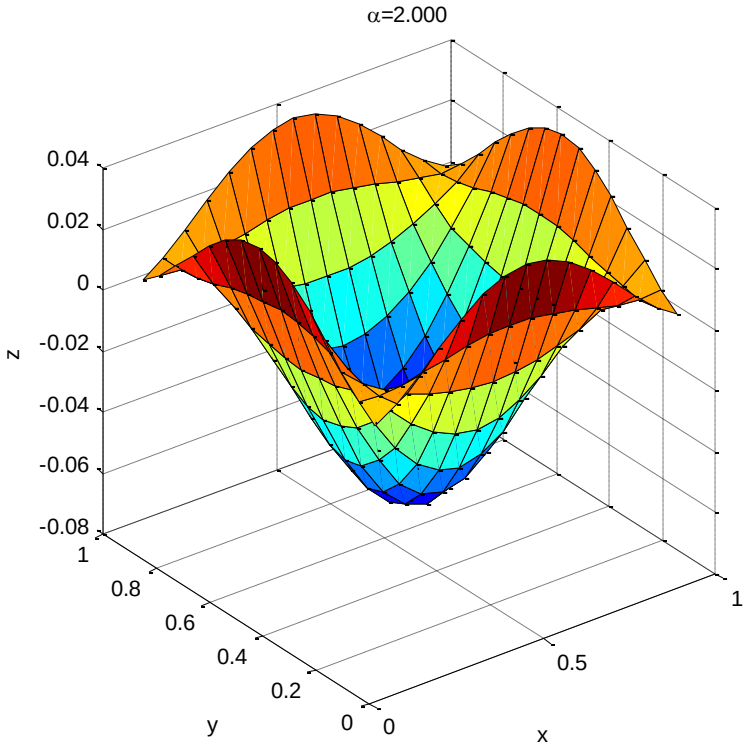

Fig.3. Surface plot of $z = 0.5\Delta\varphi(x, y)$.

in which Q_{ij} is ${}^{*}D_M^{\alpha}\varphi(i/16, i/16)$ evaluated by the 5-point GJL rule and the 8-point GL rule (for each subinterval of θ) whilst $0.5\Delta\varphi(i/16,j/16)$ is derived analytically. The difference reduces from 1.79e-1 to 1.86e-7 when $\alpha - 2$ varies from -10^{-1} to -10^{-7} as listed in Table 6. On the other hand, Figs.2 and 3 illustrate the closeness of ${}^{*}D_M^{1.999}\varphi(x,y)$ and ${}^{*}D_M^{2}\varphi(x,y)$. These results show that ${}^{*}D_M^{\alpha}\varphi(x,y)$ is left-continuous at α=2 and ${}^{*}D_M^{\alpha}$ can be regarded as a generalization of Laplacian.

Table 6. *Dif* between ${}^{*}D_M^{\alpha}\varphi(x,y)$ and ${}^{*}D_M^{2}\varphi(x,y)$ as α closes with 2

	$\alpha = 2 - 10^{-1}$	$\alpha = 2 - 10^{-3}$	$\alpha = 2 - 10^{-5}$	$\alpha = 2 - 10^{-7}$
Dif	1.79e-1	1.86e-3	1.86e-5	1.86e-7

5. Concluding Remarks

Gauss-Jacobi and Gauss-Jacobi-Lobatto quadrature rules are applied to the fractional directional integral by treating the weakly singular kernel as the Jacobi weight function that defines the Jacobi polynomials. The kernel is therefore removed from the integrand in the quadrature formula. This enables the rules to obtain very accurate approximants regardless of the singularity strength. In the last example in Section 4, the rules are compounded with the Gauss-Legendre rule to calculate the generalized fractional diffusion operator. As is discussed in the Introduction, the procedure is useful for computing the source term *f* in the FADE, e.g. [29]

$$ {}^{*}D_M^{\alpha}u(x,y) + f(x,y) = 0, \tag{54}$$

associated with a known solute distribution $u(x,y)$. The accurately determined source term *f* together with the boundary conditions on $u(x,y)$ can help benchmarking the performance of the present numerical schemes to solve the generalized fractional diffusion problems.

On the other hand, since the rules discussed in this paper can accurately implement the generalized fractional diffusion operator, they are useful in developing solution techniques for FADE. Our future study will focus on using these rules to solve FADE with different trial functions such as polynomials and radial basis functions.

Acknowledgement

The research is financially supported by the Hong Kong Research Grant Council (GRF grant HKU 7173 09E) , the 111 project under grant B12032, the National Basic Research Program of China (973

Project No. 2010CB832702), the National Science Funds for Distinguished Young Scholars (11125208) and the R&D Special Fund for Public Welfare Industry (Hydrodynamics, Project No. 201101014).

References

[1] D. Baleanu, K. Diethelm, E.Scalas et al, Fractional calculus: models and numerical methods (Series on complexity, nonlinearity and chaos vol. 3), World Scientific, 2012.

[2] G. Zaslavsky, Fractional kinetic equation for Hamiltonian chaos. Chaotic advection, tracer dynamics and turbulent dispersion, Phys. D 76(1994) 110-122.

[3] R. Hilfer, Applications of fractional calculus in physics, World Scientific, 2000.

[4] R.L. Bagley, P.J. Torvik, Fractional calculus - A different approach to the analysis of viscoelastically damped structures, AIAA J. 21(1983) 741-748.

[5] K. Adolfesson, M. Enelund, P. Olsson, On the fractional order model of viscoelasticity, Mechanics of Time-dependent Materials, 9(2005) 15-34.

[6] M. Raberto, E. Scalas, F. Mainardi, Waiting-times and returns in high-frequency financial data: an empirical study, Physica A 314(2002) 749-755.

[7] L. Sabatelli, S. Keating, J. Dudley et al, Waiting time distributions in financial markets, Eur. Phys. J.B 27(2002) 273-275.

[8] W. Chen, S. Holm, Modified Szabo's wave equation models for lossy media obeying frequency power law, J. Acoust. Soc. Am. 114(2003) 2570-2574.

[9] S. Holm, R. Sinkus, A unifying fractional wave equation for compressional and waves, J. Acoust. Soc. Am. 127(2010) 542-548.

[10] R.R. Nigmatullin, D. Baleanu, The derivation of the generalized functional equations describing self-similar processes, Fractional Calculus and Applied Analysis 15(2012) 718-740.

[11] D.A. Benson, S.W. Wheatcraft, M.M. Meerschaert, Application of a fractional advection-dispersion equation, Water Resour. Res. 36 (2000) 1403-1412.

[12] D.A. Benson, S.W. Wheatcraft, M.M. Meerschaert, The fractional-order governing equation of Lévy motion, Water Resour. Res. 36 (2000) 1413-1423.

[13] M.M. Meerschaert, D.A. Benson, B. Baumer, Multidimensional advection and fractional dispersion, Phys. Rev. E 59 (1999) 5026-5028.

[14] M. Herzallah, D. Baleanu, Existence of a periodic mild solution for a nonlinear fractional differential equation, Computers & Mathematic Applications 64(2012) 3059-3064.

[15] M.M. Meerschaert, J. Mortenson, Vector Grünwald formula for fractional derivatives, Fract. Calc. Appl. Anal. 7 (2004) 61-81.

[16] C. Monegato, A note on extended Gaussian quadrature rule, Mathematics of computation 30 (1976) 812-817.

[17] I. Podlubny, Fractional Differential Equations: An introduction to Fractional Derivatives, Fractional Differential Equations, to methods of their Solution and some of their Applications, ACADEMIC PRESS, 1999.

[18] V.J. Ervin, J.P. Roop, Variational solution of fractional advection diffusion equation on bounded domains in $\mathbb{R}^d$, Numerical methods for partial differential equations 23 (2006) 256-281.

[19] S.G. Samko., A.A. Kilbas, and O.I. Marichev, Fractional Integrals and Derivatives: Theory and Applications, Gordon and Breach, Newark, N.J., 1993.

[20] A.A. Kilbas., H.M. Srivastava, J. J. Trujillo, Theory and Applications of Fractional Differential Equations, Elsevier B.V., 2006.

[21] G.H. Golub, J.H. Welsch, Calculation of Gauss quadrature rule, Technical Report, No. CS 81, 1967.

[22] H. Wilf, Mathematics for the Physical Sciences, John Wiley and Sons, New York, 1962.

[23] G.H. Golub, Some modified matrix eigenvalue problems, SIAM Review 15 (1973) 318-334.

[24] W. Gautschi, High-order Gauss-Lobatto formulae, Numerical Algorithm 25 (2000) 213-222.

[25] Z.S. Zheng, G.H. Huang, Computation for Jacobi-Gauss Lobatto quadrature based on derivative relation, Poster, Proceedings of Modeling in Geosciences, 2010.

[26] S.J. Yang, Gauss-Radau and Gauss-Lobatto formulae for the Jacobi weight and Gori-Micchelli weight functions, Journal of Zhejiang University – Science A 3 (2002) 455-460.

[27] W. Gander, W. Gautschi, Adaptive quadrature-revisited, BIT 40 (2000) 084-101.

[28] L.F. Shampine, Vectorized adaptive quadrature in MATLAB, Journal of Computational and Applied Mathematics, 211 (2008) 131-140.

[29] J.P. Roop, Computational aspects of FEM approximation of fractional advection diffusion equations on boundary domains in $\mathbb{R}^2$, J. Comput. Appl. Math. 193(2006) 243-268.

[30] W. Chen, S. Holm, Fractional Laplacian time-space models for linear and nonlinear lossy media exhibiting arbitrary frequency power-law dependency, J. Acoust. Soc. Am. 115(2004) 1424-1430.